Simulation of Floodplain Inundation Dynamics with a High Resolution Global River Routing Model

JA-47

Dai YAMAZAKI[1*] , Taikan OKI [1], Shinjiro KANAE[2]

[1]Institute of Industrial Science, the University of Tokyo, Japan
[2] Department of Civil and Environmental Engineering, Tokyo Institute of Technology, Japan
(*Correspondence to Dai YAMAZAKI: yamadai@rainbow.iis.u-tokyo.ac.jp)

(1) INTRODUCTION

Terrestrial water circulation is important both as a component of the climate system and as a freshwater supplying system for human beings. **Global river routing models** are practically the only available tool for simulating terrestrial water circulation, however they have not adequately represented the physical mechanism of terrestrial water storage and movement, such as floodplain inundation dynamics regulated by much smaller-scale topography than global model resolution.

The **Catchment-based Macro-scale Floodplain model (CaMa-Flood)** proposed in this research overcomes this drawback by enabling higher resolution approach and explicit representation of sub-grid topography, and realized explicit representation of floodplain inundation dynamics. Ability of CaMa-Flood is tested by comparing simulated river discharge and inundated area extent with *in-situ* and satellite observations.

(2) MODEL FRAMEWORK

CaMa-Flood is a distributed river routing model which is forced by LSM runoff and simulates water storage, inundated area, river discharge, etc.

Parameter	Channel Elevation	Z
	Channel Length	L
	Channel Width	W
	Embankment Height	B
	Catchment Area	A
	Floodplain Elevation Profile	$f(Topography)$
Variables	River Storage	S_r
	Floodplain Storage	S_f
	River Water Depth	H_r
	Floodplain Depth	H_f
	Inundated Area	A_f

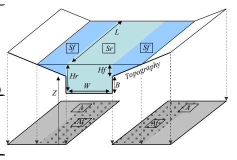

[2-1] River channel and floodplain storages are defined as continuative reservoirs in each grid. Total water storage in each grid is divided into river channel and floodplain storage to balance water surface elevation of both reservoirs.

[2-2] Water flux between grids is only considered along with prescribed River Networks. Flux calculation is done separately for river channel and floodplain in order to consider the difference of water depth and surface roughness in both reservoirs.

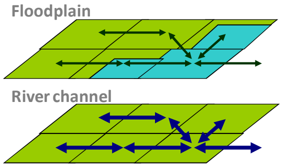

Cross-section Depth	h	Flow Velocity	v
Riverbed Slope	i_0	Discharge	Q
Water Surface Slope	$i_{sfc}=dh/dx+i_0$	Forcing Runoff	R
Manning Coefficient	n		

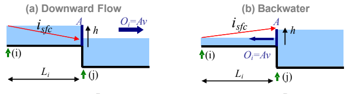

$$\frac{1}{g}\frac{\partial v}{\partial t}+\frac{v}{g}\frac{\partial v}{\partial x}+\frac{\partial h}{\partial x}+i_0-i_f=0$$

Dynamic
Diffusive
Kinematic

St. Venant Momentum Equation

$$i_f=n^2v^2h^{-\frac{4}{3}}$$

Manning Friction Slope

$$S_i(t+\Delta t)=S_i(t)+\sum_j^{upstream}Q_j\Delta t-Q_i\Delta t+A_iR_i\Delta t$$

Continuative Equation

[2-3] Diffusive Wave Equation is adopted for governing equation to represent backwater effect. Friction slope is estimated with Manning Equation, and manning coefficient is set to 0.1 and 0.3 for river channel and floodplain, respectively.
Water storage in next time step is predicted by Continuative Equation using inflow from upstream, outflow to downstream, and forcing runoff from LSM.

(3) REPRESENT SUB-GRID TOPOGRAPHY

River Networks and sub-grid topographies are objectively extracted from fine-resolution (1km) flow direction map and DEM using FLOW method [Yamazaki, 2009].

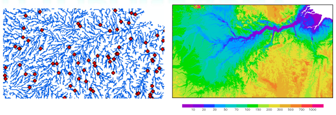

GDBD Flow Direction [Masutomi, 2009] SRTM30 DEM [NASA]

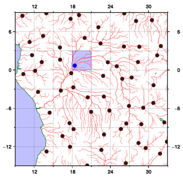

[3-1] A specific pixel of flow direction map is chosen as the "outlet pixel" of each coarse-resolution cell. Channel Elevation is decided as the elevation of the outlet pixel.

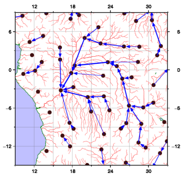

[3-2] Fine-resolution flow path is traced from the outlet pixel until the next outlet pixel is reached. This reached cell is decided as downstream, and thus River Networks are constructed.

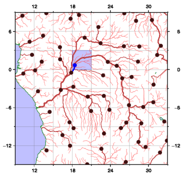

[3-3] River Channel Length is measured along with the fine-resolution flow path considering meandering at sub-grid scale.

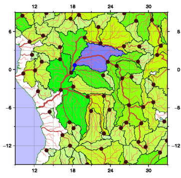

[3-4] Group of pixels which is drained into the outlet pixel is decided as "catchment pixels" of that cell. Catchment Area is decided according to the realistic boundaries based on fine-resolution dataset

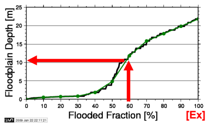

[Ex] Water depth is 10m when 60% of the catchment area is inundated

[3-5] Elevation of catchment pixels is sorted to create a virtual cross-section of the floodplain. This Floodplain Elevation Profile is used to objectively describe the relation among floodplain water storage, floodplain water depth, and inundated area.

[3-6] Channel Width and Channel Embankment Height, which are not resolved even in those fine-resolution dataset, are decided empirically.

Annual Discharge $\overline{Q}$

$$W=\max[10.0,10.0\times\overline{Q}^{0.5}]$$
$$B=\max[1.0,1.0\times\overline{Q}^{0.15}]$$

(4) SIMULATION & RESULTS

Simulation of river discharge and floodplain inundation is executed with CaMa-Flood. Primary results for Amazon River basin are validated against *in-situ* and satellite observations.

[4-1] SIMULATION SETTINGS

To evaluate impacts of introducing floodplain storage and diffusive wave equation, three sets of experiment are carried over.

Experiment	Storage	Flow Routing
NoFLD	River Channle Only	Kinematic Wave
FLD+Kine	River Channel + Floodplain	Kinematic Wave
FLD+Diff	River Channel + Floodplain	Diffusive Wave

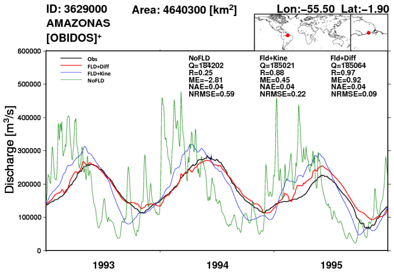

[4-2] DAILY RIVER DISCHARGE

Simulated daily river discharge is validated against GRDC **observation discharge (OBS)** at Obidos. Fluctuation of river discharge by **NoFLD** is quite large compared to other experiments and observation. This implies that floodplain has a role to smooth discharge variance by storing water spilled out from river channel. Result by **FLD+Diff** shows better fit to **observation** than that of **FLD+Kine**.

[4-3] FLOW VELOCITY

Simulated Flow Velocity by **FLD+Diff** and **FLD+Kine** are compared in high water season of Amazon (May). Flow velocity by **FLD+Diff** is slower in branches of Amazon River (Circled). This is because Diffusive Wave can represent backwater effect (i.e. flow stagnation due to water level rise in main stream). Representation of backwater effect may lead to the improved river discharge simulation by **FLD+Diff**.

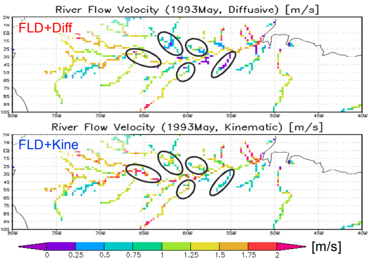

[4-4] INUNDATED AREA

Simulated Inundated Area by **FLD+Diff** is validated against **satellite observation** by Prigent [2007]. Model is overestimating inundated area in upper Amazon River basin in high water season, but overall spatial pattern of inundated area is almost similar to the observation.

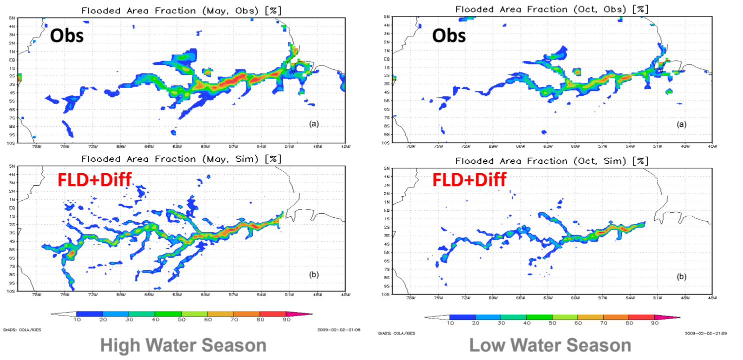

Temporal variation of simulated inundated area is also compared with **satellite observation** for Amazon River Central Floodplains. Model can predict the average and seasonal variation of inundated area at a certain level, even though predicted inundation peak is one month earlier than observation.

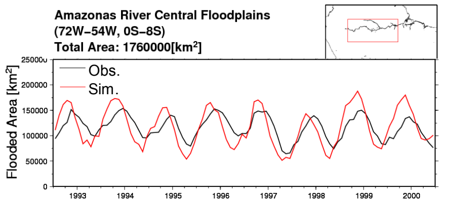

(5) CONCLUSION

Explicit representation of sub-grid topography and introduction of Diffusive Wave is achieved in **CaMa-Flood** model. Those improvements on global river routing models enables **realistic simulation of floodplain inundation dynamics**. Simulated results by CaMa-Flood shows better agreement to observations than previous river routings.

REFERENCES

Masutomi et al.: Development of Highly Accurate Global Polygonal Drainage Basin Data. *Hydrol. Proc.*, 2009
Prigent et al.: Global Inundation Dynamics Inferred from Multiple Satellite Observations, 1993-2000. *J. Geophys. Res.*, 2007
Yamazaki et al.: Deriving a global river network map at flexible resolutions from a fie-resolution flow direction map with explicit representation of topographical characteristics in sub-grid scale, *Hydrol. Earth Syst. Sci. Discuss.*, 2009.

ACKNOWLEDGEMENTS

The first author is supported by a Research Fellowship from Japan Society for the Promotion of Science (JSPS). This research is partly supported by the Innovative Program of Climate Change Projection for the 21st Century (KAKUSHIN Program) by the Japanese Ministry of Education, Culture, Sports, Science, and Technology. We especially appreciate Dr. Prigent for providing her latest observation datasets.

Sixth International Scientific Conference on the Global Energy and Water Cycle @ Melbourne, Australia 24-28 August 2009 GEWEX & iLEAP Joint Session A